

Monitoring of artificial infiltration using electrical resistivity method

Hiroomi Nakazato¹, Seiichiro Kuroda¹, Takehiko Okuyama¹, Mutsuo Takeuchi¹,
Mikyung Park², and Hee Joon Kim²

¹National Institute for Rural Engineering, Tsukuba, Japan, ²Pukyong National University, Pusan, Korea

Abstract: A infiltration experiment of river water has been conducted to evaluate the applicability of electrical resistivity monitoring methods in an area containing gravelly deposits in Nagaoka, Japan. Apparent resistivity data, which are inverted to obtain the resistivity distribution, are measured with a newly developed system. This system can collect 490 data in an hour and be controlled with PC to store the data. Subsurface resistivity sections, which are obtained from two-dimensional nonlinear inversion of time-lapse apparent resistivity data, enable us to estimate the direction of the flow and the rate of infiltration. The infiltration rate is estimated to be 4.4×10^4 m/s in the early stage of the experiment when the infiltration process is dominant.

1. Introduction

In recent years, organochlorine and nitrate-nitrogen pollution of the ground has become a serious environmental problem. The flow of groundwater contributes greatly to the movement of pollutants. To explain and predict the mechanisms of geo-environmental pollution, it is necessary to have a method that can economically investigate over a wide area the heterogeneous geological structure that governs groundwater flow and the movement of pollutants and groundwater. The resistivity of the ground depends upon the degree of saturation with water, the porosity, and the resistivity of the porewater (Archie, 1942). In unsaturated areas the flow of groundwater varies the resistivity of the ground with the degree of saturation. In saturated areas, however, the resistivity of the ground mainly depends on that of porewater accompanying the flow of groundwater.

This research examines the method of electrical resistivity prospecting using continuous electrical measurement as a means of monitoring groundwater flow in the geo-environment. The applicability of the method was studied with an artificial groundwater infiltration test, using the recharge water as a tracer to clarify groundwater flow.

2. Research Test Method

Outline of the test site

The test site is located in Takateramachi, Nagaoka City, Niigata Prefecture (Fig. 1). The test site is geomorphologically a high terrace surface, inclining towards the northwest.



Fig. 1. Location map showing test site and remote electrodes.

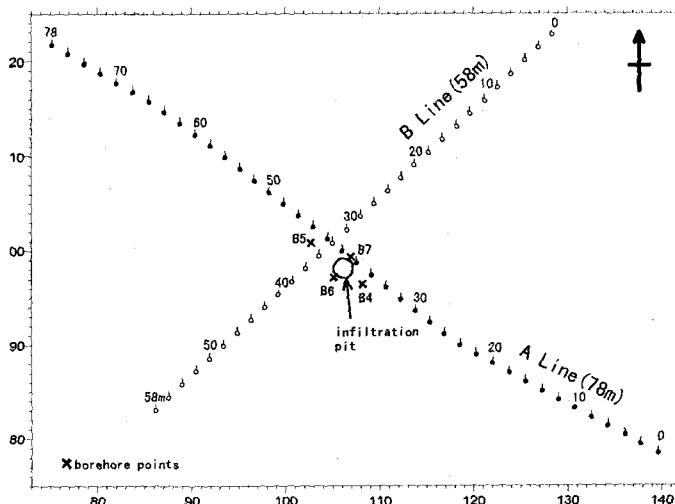


Fig. 2. A map showing survey lines, boreholes and infiltration pit.

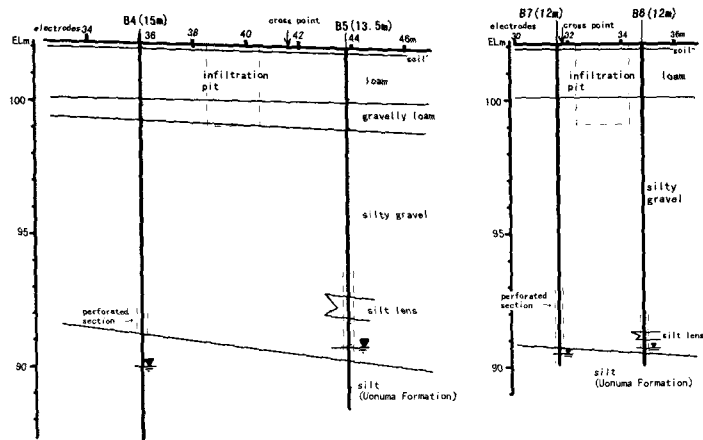


Fig. 3. Geological section along A-Line. Fig. 4. Geological section along B-Line.

The geology of the test site is, in ascending order, a silt layer, a silty gravel layer, a gravelly loam layer (in Figure 4 it is shown together with the silty gravel layer), a loam layer, and a soil layer (Figs. 3 and 4). The lowest silt layer is thought to be the Uonuma Formation, effectively an impervious basement in the test site. The layers above the silt layer are terrace deposits, the silty gravel layer is 8.7 m thick, the base of which is tilted 7° to 17° in the westerly direction. Near the bottom of boreholes B5 and B6 there is a silt lens of 0.3 to 0.8 m thick. The thickness of the gravelly loam layer is 0.6 to 0.9 m. The loam layer together with the soil layer is approximately 2 m thick.

According to records of the water level in borehole B5 from September 1999 to November 2001, the groundwater level in the test site during the period of accumulation and melting of snow from December to April reaches as high as the elevation of 97 m. However, after April the level is generally below 92.5 m (Hokuriku Regional Agricultural Administration Office, 2002). Prior to the implementation of the test on 11th October 2001 there was no rainfall on or after 1st October, so the water level was stable at 90.8 m. The base of the silty gravel layer is at 90.3 m, so it can be inferred that at the start of the infiltration test the majority of the silty gravel layer was unsaturated. The hydraulic conductivity of the silty gravel layer is in the range of $k = 2.7 \times 10^{-3}$ to 9.4×10^{-5} m/s (Hokuriku Regional Agricultural Administration Office, 2002).

The recharge facility was a cylindrical-shaped infiltration pit, 2.0 m diameter by 3.0 m deep. The wall surface was protected by a liner plate. The depth of the bottom corresponded to the base of the gravelly loam layer. A 20cm layer of gravel was laid on the bottom to act as a filter.

Test method

Using crosshole radar on this test site, Kuroda et al. (2002) estimated the downward movement of the infiltration front of recharge water to be 8×10^{-4} m/s. From this velocity it was estimated that the time for the recharge water to reach the groundwater level from the bottom of the infiltration pit was three hours. To monitor the rapid movement by means of a repeated two-dimensional resistivity prospecting method, it is necessary to employ multi-channel receivers together with a pole-pole electrode arrangement (Nakazato et al., 2002). In this research there were two survey lines at right angles on the surface (A-Line: 78m long with 40 electrodes, and B-Line: 58m long with 30 electrodes). For each line, pole-pole resistivity data could be efficiently obtained using a three-channel monitoring equipment. With this system, a pseudosection with 406 data could be obtained in approximately 50 minutes for A-Line, while that with 225 data in approximately 25 minutes for B-Line. Also, the monitoring equipment (McOHM21; Oyo Corporation) was improved to be capable of long hours of continuous monitoring. A block diagram of the monitoring system is shown in Figure 5.

In the infiltration test carried out on 11th October, 2001, a total of 20 m³ of river water was recharged over the 8-hour period from 11:00 to 19:00. The water temperature in each borehole was 12.5 to 14 °C, with an electrical conductivity of 20 to 30 mS/m (resistivity of 50 - 33 Ωm), and the recharge water temperature was an average of 19.5 °C, with an electrical conductivity of 12.6 mS/m (79.4 Ωm). One set of resistivity monitoring measurements consisted of twice on A-Line and once on B-Line. Before the infiltration test a set of background measurements was taken, and during the infiltration test 6 sets of measurements were taken (Fig. 6). There was no rainfall during the resistivity monitoring period.

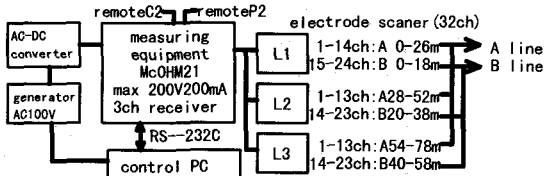


Fig. 5. Arrangement of survey equipments.

To investigate the change in the resistivity distribution with time, inversion is normally carried out at each individual survey cross-section to obtain a change ratio relative to the initial value for each sub-divided small area. However, in each individual inversion result there are differences in the noise component added to the true resistivity change, and the convergence is slightly different. As a result, the likelihood is high that the noise component will have majority of the inverted resistivity difference. Sugimoto (1995) proposed a resistivity change ratio inversion method that takes into account the non-linearity of the resistivity changes. As a summary of the method, firstly the measured difference data is added to the theoretical data calculated from a suitable reference cross-section (normally the results of inverting the initial data values are used), and inversion is carried out. The resistivity change ratio is then obtained from the difference between the derived resistivity distribution and the resistivity distribution on the reference cross-section. Sugimoto (1995) showed that still more accurate analysis was possible using this method by constraining the direction of the resistivity change.

Because the resistivity declines when recharging into an unsaturated region, in accordance with Sugimoto's method the analysis is carried out with the resistivity decreasing relative to the background value. Both the inversion to obtain the resistivity cross-section from the background data and the inversion to obtain the time series cross-sections of the resistivity change ratio were carried out with E-Tomo v.4.0 (DIA Consultants Co., Ltd.), using the non-linear least squares method with initial constraints.

3. Results

Background data analysis

The cross-sections of resistivity on A- and B-Line from the background measurements are shown in Figure 7. The RMS error of the measured apparent resistivity value, ρ_{off} , and the apparent resistivity value calculated from the inverted resistivity distribution model, ρ_{aci} , is an index that indicates the validity of the analysis results, and is obtained from the following formula:

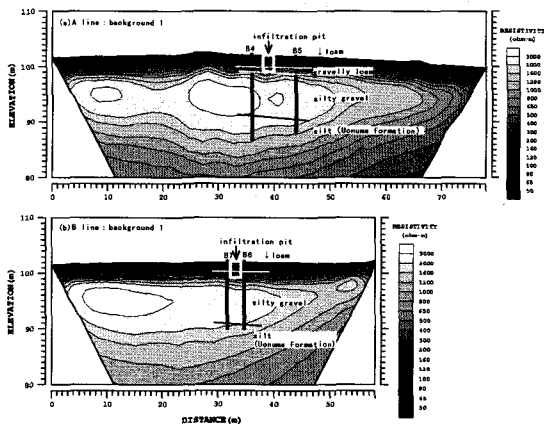


Fig. 7. Interpreted resistivity sections along A- (upper) and B-Line (lower).

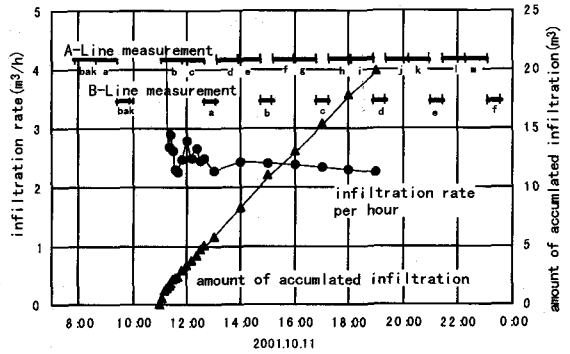


Fig. 6. Plan of infiltration test and survey program.

As a result, the likelihood is high that the noise component will have majority of the inverted resistivity difference. Sugimoto (1995) proposed a resistivity change ratio inversion method that takes into account the non-linearity of the resistivity changes. As a summary of the method, firstly the measured difference data is added to the theoretical data calculated from a suitable reference cross-section (normally the results of inverting the initial data values are used), and inversion is carried out. The resistivity change ratio is then obtained from the difference between the derived resistivity distribution and the resistivity distribution on the reference cross-section. Sugimoto (1995) showed that still more accurate analysis was possible using this method by constraining the direction of the resistivity change.

Because the resistivity declines when recharging into an unsaturated region, in accordance with Sugimoto's method the analysis is carried out with the resistivity decreasing relative to the background value. Both the inversion to obtain the resistivity cross-section from the background data and the inversion to obtain the time series cross-sections of the resistivity change ratio were carried out with E-Tomo v.4.0 (DIA Consultants Co., Ltd.), using the non-linear least squares method with initial constraints.

Table 1. Variation of RMS misfits during inversion iterations. The lower-case letters of a – m indicate the periods shown in Fig. 6.

A	bak	a	b	c	d	e	f	g	h	i	j	k	l	m
0	49.76	0.42	0.42	0.57	0.62	0.82	0.92	0.88	1.09	1.12	1.19	1.10	1.05	1.02
1	14.21	0.40 ^a	0.33 ^a	0.46 ^b	0.41 ^b	0.58 ^c	0.55 ^c	0.39 ^d	0.58 ^e	0.51 ^e	0.50 ^f	0.48 ^f	0.43 ^g	0.49
2	4.80	0.40 ^a	0.33 ^a	0.46 ^b	0.41 ^b	0.58 ^c	0.55 ^c	0.39 ^d	0.58 ^e	0.51 ^e	0.50 ^f	0.48 ^f	0.43 ^g	0.49
3	1.40	0.40 ^a	0.33 ^a	0.46 ^b	0.41 ^b	0.58 ^c	0.55 ^c	0.39 ^d	0.58 ^e	0.51 ^e	0.50 ^f	0.48 ^f	0.43 ^g	0.49
4	0.92	0.40 ^a	0.33 ^a	0.46 ^b	0.41 ^b	0.58 ^c	0.55 ^c	0.39 ^d	0.58 ^e	0.51 ^e	0.50 ^f	0.48 ^f	0.43 ^g	0.49
5	0.63	0.40 ^a	0.33 ^a	0.46 ^b	0.41 ^b	0.58 ^c	0.55 ^c	0.39 ^d	0.58 ^e	0.51 ^e	0.50 ^f	0.48 ^f	0.43 ^g	0.49
6	0.48	0.40 ^a	0.33 ^a	0.46 ^b	0.41 ^b	0.58 ^c	0.55 ^c	0.39 ^d	0.58 ^e	0.51 ^e	0.50 ^f	0.48 ^f	0.43 ^g	0.49

B	bak	a	b	c	d	e	f
0	32.13	0.31	0.62	0.87	1.12	1.11	0.95
1	14.3	0.24 ^a	0.28 ^a	0.41 ^b	0.35 ^b	0.36 ^b	0.36
2	7.67	0.24 ^a	0.28 ^a	0.41 ^b	0.35 ^b	0.35 ^b	0.36
3	4.77	0.24 ^a	0.28 ^a	0.41 ^b	0.35 ^b	0.35 ^b	0.36
4	3.12	0.24 ^a	0.28 ^a	0.41 ^b	0.35 ^b	0.35 ^b	0.36
5	1.65	0.24 ^a	0.28 ^a	0.41 ^b	0.35 ^b	0.35 ^b	0.36
6	1.03	0.24 ^a	0.28 ^a	0.41 ^b	0.35 ^b	0.35 ^b	0.36

$$RMS_{error} = \sqrt{\sum_{i=1}^N (\ln \rho_{afi} - \ln \rho_{aci})^2 / N} \times 100 \text{ (\%)} \quad (1)$$

The RMS errors for each analysis for 6 inversion iterations were 0.48% on A-Line, and 1.03% on B-Line (Table 1), indicating a high validity for the analysis results. Each cross-section shows a three-layer structure, corresponding to the underlying geological structure. The surface layer with resistivity less than 500 Ωm is the loam layer, the layer underneath with high resistivity 500 to 3000 Ωm is the silty gravel layer, and the lowest layer with low resistivity 1200 to 2000 Ωm corresponds to the Uonuma silt layer.

Resistivity change ratio analysis

The ratio of resistivity change at a particular time, d_t , is defined in terms of the background interpreted resistivity value before the infiltration test, R_0 , and the interpreted resistivity value at each time, R_t , for each small element of ground, as follows:

$$d_t \text{ (\%)} = (R_t - R_0) / R_0 \times 100 \quad (2)$$

Cross-sections of the resistivity change ratio are shown in Figures 8 and 11. For both measurement lines the cross-sections show ± 20 m in the horizontal direction on either side of the projected position of the infiltration pit, and as far as elevation 80 m in the depth direction. The scale of the change ratio is uniformly 0% to -10% in 0.5% increments. Looking at all the RMS errors for the resistivity change ratios, convergence was achieved on the second iteration, and they are all less than 1% (Table 1). Therefore it can be concluded that differences in the order of 1% in the resistivity change ratio are significant. The following are discussions for each measurement line.

The resistivity change ratio distribution for the two background measurements is shown in Figure 8-a. All points are in the range 0% to -1%, from which it can be confirmed that the accuracy of this analysis system is within 1%.

Looking generally at the reduction in resistivity, firstly at the location of the infiltration pit, a resistivity change ratio of greater than -10% that becomes more evident with the passage of time can be recognized. In other locations, the maximum change ratio is in the range of -3.5% to -4.0%. The expansion of the region of decreased resistivity in the depth direction can be seen in Figures 8-b to 8-f, and thereafter an expansion of the region of decreased resistivity, represented by the -2.5% contour, in the direction of the end points of the measurement can be recognized.

Regarding the resistivity change ratio in the depth direction, the groundwater level directly underneath the infiltration pit prior to the start of the infiltration test was postulated to be at elevation 91 m, from the water levels in boreholes B5 and B7. The resistivity change ratio at this point in each measurement is read from Figure 8 to arrive at Figure 9. From Figure 9 it can be seen that at the water level point directly underneath the infiltration pit, the resistivity declined steadily until for 5 hours from the start of recharging; thereafter it remained almost constant. Taking the time for the main body of recharge water to percolate from the bottom of the infiltration pit to the groundwater level from the start of recharging as 5 hours, and the distance from the bottom of the infiltration pit (elevation 99 m) to the groundwater level as 8 m, the apparent permeation velocity of the recharge water can be calculated to be 4.4×10^{-4} m/s.

Regarding the resistivity change in the direction of the measurement end points, if the distance from the center of the infiltration pit to the point on the -2.5% contour furthest towards the measurement end points is plotted against measurement time, Figure 10 is obtained. Excluding the values from Figures 8-g and 8-h, there is a point of inflection at about 4 hours after the start of recharging; after 4 hours the speed of movement of the contour increases, then after 8 hours, after recharging has stopped, the speed of propagation becomes smaller than before.

The cross-sections of resistivity change ratio on B-Line are from measurement results at approximately two-hourly intervals. Also, in contrast to Line A, which passed through the infiltration pit, B-Line passed through a point 2 m from the infiltration pit on the downstream side of the slope. Unlike A-Line, a distinct decline in the resistivity near the surface was not observed. As in A-Line, looking at the change in the resistivity change ratio with time at the point at elevation 91 m below the infiltration pit, resistivity declined during the 8-hour recharging period it was almost constant between 8 and 10 hours, and thereafter resistivity began to increase (Fig. 9). The 2 points up to 4 hours are plotted at the same position as those for A-Line, indicating that the same monitoring results were obtained for the movement of recharging water after the start of recharging for both measurement lines. For B-Line, the maximum value of resistivity change ratio is greater than that for A-Line. This is thought to be because on A-Line the permeation of recharge water includes a component in the direction down stream of the slope, so that on B-Line, which is positioned downstream of the infiltration pit, a greater resistivity change ratio is obtained.

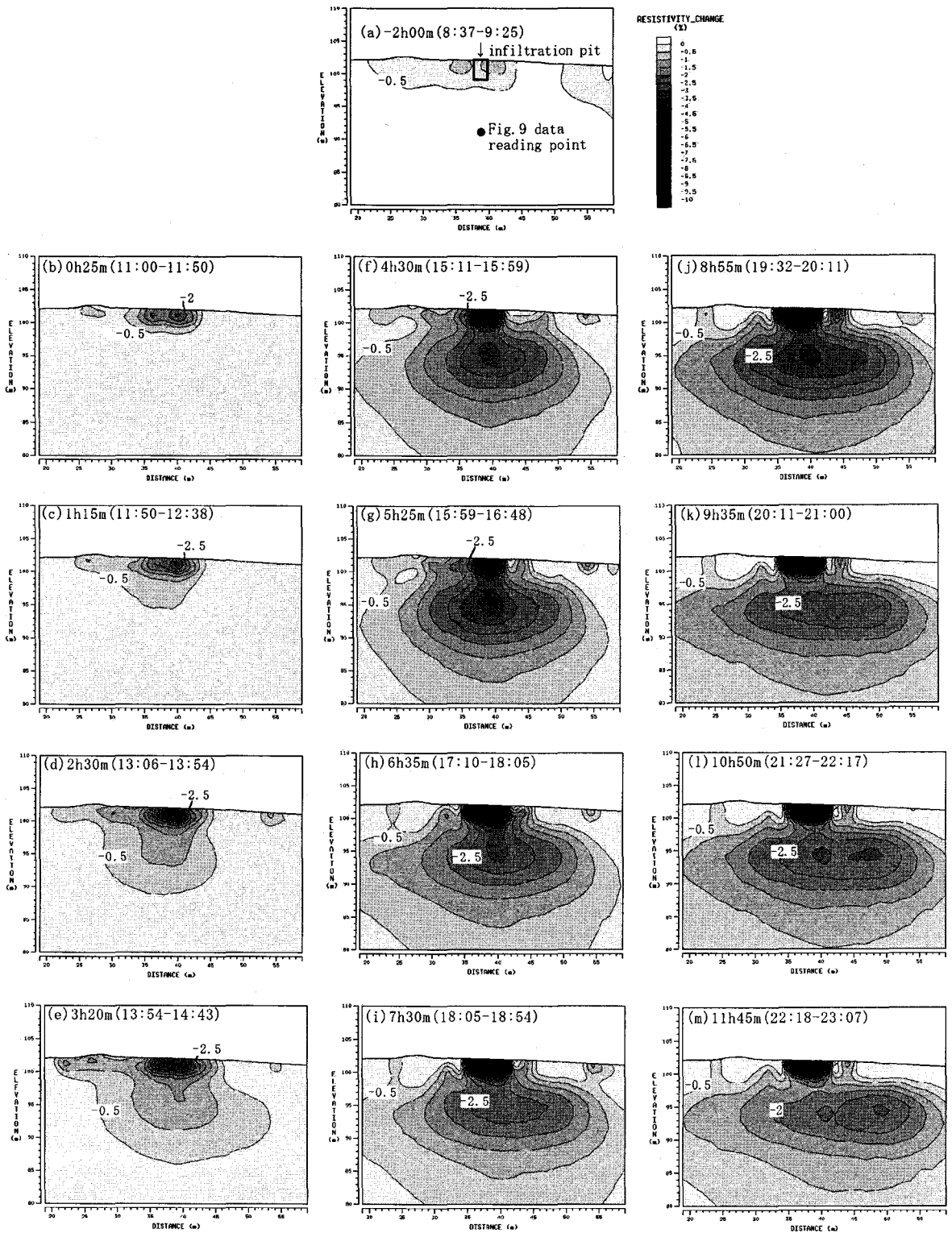


Fig. 8. Time-lapse sections of resistivity change ratio along A-Line.

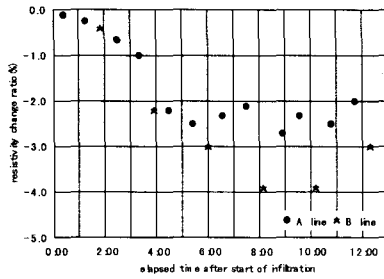


Fig. 9. Comparison of resistivity change ratios at the elevation of 90 m along A- and B-Line after water recharge.

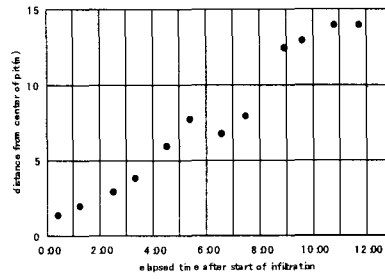


Fig. 10. Downward migration of the resistivity contour of -2.5% as a function of time after water recharge.

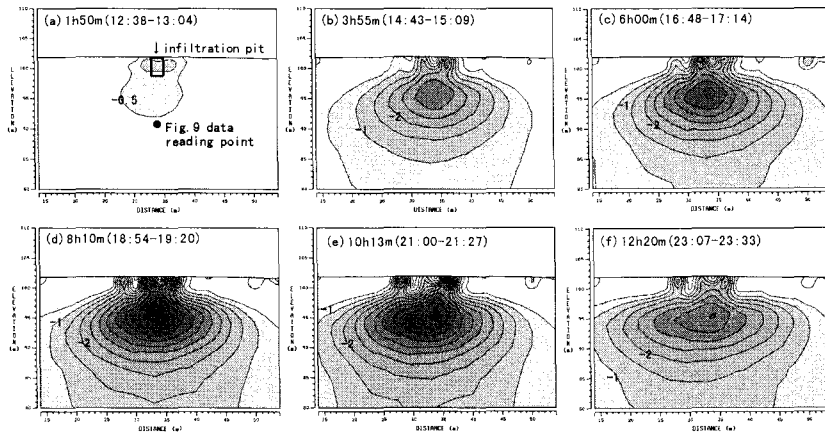


Fig. 11. Time-lapse sections of resistivity change ratio along B-Line

4. Discussion

Effect of three-dimensionality of the recharging water

It is thought that the recharging water from the bottom of the infiltration pit initially forms a cylindrically shaped body with high degree of saturation. In contrast to this, 2-D monitoring using the resistivity prospecting method assumes a 2-D structure with no change in the resistivity structure perpendicular to the underground cross-section. Because of this it is possible that changes in the resistivity caused by the movement of the recharging water mass, which is not considered to have continuity in the perpendicular direction, are not adequately represented. Also, in A- and B-Line at the position of the infiltration pit the variations with time of the resistivity change ratio are considerably different, and we consider this due to the difference in the distance from the infiltration pit to the measurement line. Because of this, to model the present test situation, we created a 3-D resistivity method modeling program, using a finite element method with tetrahedral elements based upon Sasaki (1994). Using this program, we modeled a square column with low resistivity ($10 \Omega\text{m}$) with a bottom area $2 \text{ m} \times 2 \text{ m}$ extending 2 m, 4 m, and 10 m down from the surface; this column was placed within a uniform $100 \Omega\text{m}$ half-space. Then we calculated 2-D monitoring data for the pole-pole method for the case of electrodes placed at 2 m intervals along a 78 m measurement line in contact with the square column (Measurement line 1: corresponding to A-Line) and for the case of the same line but separated from the square column by 2 m (Measurement line 2: corresponding to B-Line) (Fig. 12). Next, for each data, using the uniform $100 \Omega\text{m}$ half-space as the initial values,

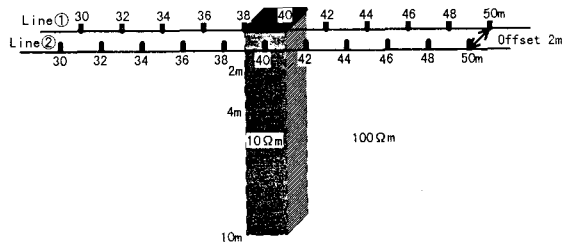


Fig. 12. A model showing a square pillar of $10 \Omega\text{m}$ in a homogeneous half-space of $100 \Omega\text{m}$.

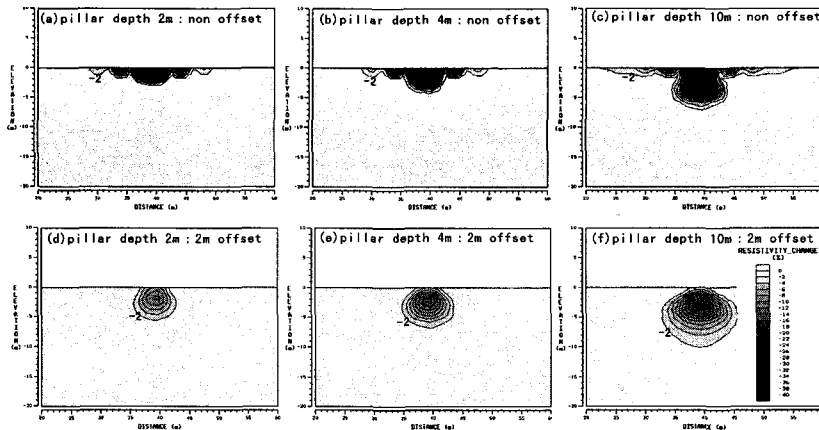


Fig. 13. Inverted sections of resistivity change ratio along lines 1 (upper) and 2 (lower) with three synthetic pole-pole data generated from three bottom depths [2 m (left), 4 m (middle), and 10 m (right)] of the square pillar shown in Fig. 12.

we carried out a back-analysis for resistivity change ratio to the same specifications as the data measured on site, and derived the resistivity change ratio distribution (Fig. 13).

The results showed that the resistivity change ratio distribution differed greatly depending upon the positional relationship between the low resistivity square column and the measurement line. This confirmed that the reason for the difference in the analysis results for A- and B-Line was the size of the offset of the infiltration pit from the measurement line. When the low resistivity square column was in contact with the measurement line there was a tendency for the reduction in surface resistivity to be amplified as the depth of the low resistivity square column increased. The increasing depth of the low resistivity square column was expressed as an expansion of the region showing a several percent reduction in surface resistivity; however, the region of reduced resistivity did not extend as far down as the bottom of the low resistivity square column. When there is an offset between the low resistivity square column and the measurement line, there is a tendency for the region of reduced resistivity, with concentric contours, to expand in the depth direction as the depth of the low resistivity square column increases. However, even when the bottom of the column is 10 m deep, the depth of the center of the reduced resistivity region is 3 m, and the resistivity change ratio at 10 m depth is no more than -2%. These results indicate the limitations of applying 2-D monitoring to a 3-D structure.

It can be seen from Figures 8 and 11 that there is no tendency for the reduced resistivity region to extend below elevation of 90 m. As elevation of 90 m corresponds to the elevation of the top surface of the impermeable basement, it is considered that the reduced resistivity region reflects to a certain extent the actual movement of the changing water. However, when applying the resistivity method using 2-D monitoring to 3-D time-series change phenomena, it is necessary to consider the change in shape of the reduced resistivity region of the 2-D cross-section as an apparent phenomenon. Furthermore, it is important not to consider the resistivity change ratio at the position of the low resistivity square column from the analysis as being the actual resistivity change ratio.

Applicability of the continuous resistivity prospecting method to geo-environment monitoring

In boreholes B4 and B5 there was a tendency for the water level to decrease during the infiltration test, because water samples were taken during the test. However, in boreholes B6 and B7, which are near the infiltration pit, an increase in the water level was observed 4 to 5 hours after the start of recharging (Fig. 14). If this is taken as the time when the recharging water arrived at the surface of the groundwater from the bottom of the infiltration pit, the permeation velocity is virtually the same as the apparent permeation velocity obtained from the resistivity change ratio distribution diagrams. In the present geo-environmental monitoring using the continuous electrical resistivity

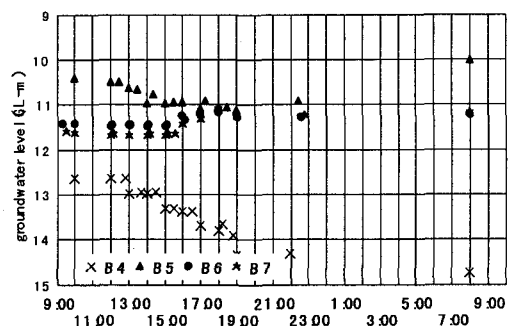


Fig. 14. Groundwater levels in boreholes (Oct.11-12,2001).

method there is a problem of using a 2-D analysis for a 3-D phenomenon. However, it can be concluded nevertheless that highly valid results were obtained.

5. Conclusions

We investigated the applicability of continuous electrical resistivity measurements to geo-environment monitoring from a case study of an artificial infiltration test, and obtained the following results.

- (1) The direction and the movement of the flow of the recharging river water were monitored with time-lapse subsurface electrical resistivity imaging. Apparent resistivity data, which were inverted to obtain the resistivity distribution, were measured with a newly developed system. This system can collect 490 data in an hour and be controlled with PC to store the data.
- (2) It was possible to accurately obtain the time-lapse resistivity reduction associated with the recharging by using constrained, non-linear inversions of the resistivity change ratios. The apparent infiltration rate was estimated to be 4.4×10^{-4} m/s in the early stage of the experiment when the infiltration process was dominant.
- (3) By using a 3-D modeling program, 2-D survey data were calculated for a 3-D resistivity structure, and resistivity change ratio analysis was carried out to model the permeation of recharge water. The results showed that the distribution of resistivity change ratio is very dependant upon the distance from the infiltration pit to the survey line. Also, only a small amount of resistivity change was detected in the deep region.
- (4) The model results indicated that when inferring changes in the geo-environment from resistivity change ratios from 2-D analysis, it is necessary to consider whether the object of the investigation is a 2-D structure or not.
- (5) The apparent permeation velocity estimated from resistivity measurements agreed with the permeation velocity obtained from changes in the groundwater level associated with the recharging. Also, we confirmed the validity of the 2-D survey method for 3-D permeation of recharging water.

References

- Archie, G.E., 1942, The electrical resistivity log as an aid in determining some reservoir characteristics, *Trans. AIME*, 146, 54–62.
- Hokuriku Regional Agricultural Administration Office, 2002, Report on groundwater survey method improvements in the Uonuma terrace region, 295 p, Hokuriku Regional Agricultural Administration Office.
- Kuroda, S., Nakazato, H., Nihira, S., Hatakeyama, M., Takeuchi, M., Asano, M., Todoroki, Y. and Konno, M., 2002, Cross-hole geo-radar monitoring for moisture distribution and migration in soil beneath an infiltration pit: a case study of an artificial groundwater recharge test in Niigata, Japan, Ninth International Conference on Ground Penetrating Radar, Koppenjan, S. K. and Lee, H. (eds), *Proc. SPIE*, 4758, 703–707.
- Nakazato, H., Hatakeyama, M., Kuroda, S., Natsuka, I., Suzuki, K., Fujita, Y. and Enami, N., 2002, Preliminary study on the resistivity monitoring using surface-subsurface electrode system, Technical report of the National Institute of Rural Engineering of Japan, 200, 129-137.
- Sasaki, Y., 1994, 3-D resistivity inversion using the finite-element method, *Geophysics*, 59, 1839–1848.
- Sugimoto Y., 1995, Electrolyte tracer monitoring using resistivity tomography – quantitative research, Society of Exploration Geophysicists of Japan, *Proceedings of the 92nd Conference*, 57–62.